Heat shock protein B7 (HSPB7) inhibits lung adenocarcinoma progression by inhibiting glycolysis

ZHITAO CHEN[1], PEIPEI LI[2], LINGGUANG SHEN[2] and XIUYU JIANG[3]

Departments of [1]Thoracic Surgery and [2]General Surgery; [3]Health Management Center, Jinan Central Hospital Affiliated to Shandong First Medical University, Jinan, Shandong 250013, P.R. China

Received May 24, 2023; Accepted September 4, 2023

DOI: 10.3892/or.2023.8633

Abstract. In the present study, it was aimed to investigate the effects and potential mechanisms of heat shock protein B7 (HSPB7) on lung adenocarcinoma (LUAD). Bioinformatic analysis was performed to explore the association between HSPB7 expression and patients with LUAD. MTT, colony formation, wound healing and Transwell assays were performed to examine the proliferative, migratory and invasive abilities of H1975 and A549 cells. Western blot analysis was conducted to determine the corresponding protein expression. Co-Immunoprecipitation and Chromatin immunoprecipitation assays were carried out to reveal the interaction between HSPB7 and myelodysplastic syndrome 1 and ecotropic viral integration site 1 complex locus (MECOM). In addition, an animal model was conducted by the subcutaneous injection of A549 cells into BALB/c nude mice, and tumor weight and size were measured. HSPB7 was downregulated in LUAD tissues and cells, and its expression level correlated with patient prognosis. Cell functional data revealed that silencing of HSPB7 promoted lung cancer cell proliferation, migration, invasion and epithelial mesenchymal transition (EMT); whereas overexpression of HSPB7 led to the opposite results. Furthermore, bioinformatics analysis showed that HSPB7 inhibited glycolysis. HSPB7 decreased glucose consumption, lactic acid production, and lactate dehydrogenase A, hexokinase 2 and pyruvate kinase muscle isoform 2 protein levels. The results demonstrated that MECOM was a transcription factor of HSPB7. Collectively, these results suggested that HSPB7 is regulated by MECOM, and that HSPB7 attenuates LUAD cell proliferation, migration, invasion and EMT by inhibiting glycolysis.

Correspondence to: Dr Xiuyu Jiang, Health Management Center, Jinan Central Hospital Affiliated to Shandong First Medical University, 105 Jiefang Road, Jinan, Shandong 250013, P.R. China
E-mail: jxx33167@163.com

Abbreviations: MDS1, myelodysplastic syndrome 1; EVI1, ecotropic viral integration site 1; MECOM, MDS1 and EVI1 complex locus; EMT, epithelial to mesenchymal transition; HK2, hexokinase 2; HSPB7, heat shock protein B7; LDHA, lactate dehydrogenase A; LUAD, lung adenocarcinoma; PKM2, pyruvate kinase muscle isoform 2

Key words: LUAD, HSPB7, MECOM, cell proliferation, cell invasion

Introduction

The global incidence and mortality rates of lung cancer remain high and the five-year survival rate has been reported to be ~20% (1-3). Lung adenocarcinoma (LUAD) is one of the most common pathological subtypes of lung cancer, accounting for ~40% of cases (4,5). Despite considerable advances in anticancer therapy, the overall survival and prognosis of patients with LUAD has not improved significantly (6,7). Therefore, an improved understanding of the drivers of LUAD and the molecular mechanisms could improve the diagnosis and treatment of this deadly disease.

Heat shock proteins act as chaperones at the molecular level and have been investigated in numerous diseases associated with oxidative stress, including obesity (8,9). A specific subfamily of heat-shock proteins are the HSPB family of molecular chaperones, which comprises ten members (HSPB1-10, also called small HSP) (10). HSPB7 is a member of the HSPB family and has been shown to be ineffective in suppressing the amorphous aggregation of model proteins, however, it is very effective in preventing the aggregation of huntingtin fragments enriched with Gln residues (11). HSPB7 is crucial for heart development as it modulates actin filament assembly (12). HSPB7 interacts with dimerized filamin C, and its absence results in progressive myopathy in skeletal muscle (13).

Other genes in the HSPB family have been associated with glycolysis. Increased glycolysis, oxidative phosphorylation, and stem cell characteristics of esophageal cancer stem-like cells depend on the Hsp27 (HSPB1)-AKT-HK2 pathway (14). The bidirectional gene HspB2/αB-crystallin may be involved in the levels of reactive oxygen species and glycolysis in MCF7 cells (15). However, the effect of HSPB7 on the expression of glycolytic enzymes and level of glycolysis has not been previously reported. It was hypothesized that HSPB7 may indirectly affect the expression of glycolytic enzymes and the level of glycolysis, but further studies are required to elucidate the molecular mechanisms by which HSPB7 participates in glycolysis.

Increasing evidence has indicated that HSPB7 acts as a tumour suppressor in a variety of malignant tumours (16,17). However, there is no study on the role of HSPB7 in LUAD. In the present study, it was hypothesized that HSPB7 participates in LUAD progression and its potential role and mechanism of action were investigated. Preliminary analysis revealed that HSPB7 was significantly downregulated in LUAD tumour tissues and cells, suggesting that it may be a candidate tumour suppressor gene in LUAD.

Materials and methods

Bioinformatics analysis. The expression profiles of myelodysplastic syndrome 1 (MDS1) and ecotropic viral integration site 1 (EVI1) complex locus (MECOM) of patients with LUAD was analysed using the Gene Expression Profiling Interactive Analysis (GEPIA) website (http://gepia2.cancer-pku.cn/#index) (18). In GEPIA website, it was not possible to acquire clinical characteristics of 483 LUAD patients. To show clinical characteristics, HSPB7 expression profiles and clinical characteristics of patients with LUAD [515 cases, International Classification of Diseases (ICD-10) (19), C34] were downloaded from TCGA (https://portal.gdc.cancer.gov/), and then analyzed via R software (version 3.6.1, https://www.r-project.org/). A survival curve for HSPB7 expression was obtained using GEPIA. The survival curve of MECOM expression was obtained from the Kaplan Meier plot (http://kmplot.com/analysis/). Survival analysis was performed using the Kaplan-Meier method, and the log-rank test was used to compare survival times between the low and high expression groups. Gene set enrichment analysis (GSEA) was used to identify HSPB7 related signaling pathways in the LUAD dataset using the following parameters: Number of permutations=1,000; permutation type=gene_set; enrichment statistic=weighted; and metric for ranking genes=Signal2Noise. The binding site of HSPB7 and MECOM was predicted using the JASPAR website (http://jaspar.genereg.net/).

Tissue collection. Between September 2020 and December 2021, 23 tumour tissues and paired normal tissues from patients with LUAD (13 males and 10 females; age range: 28-75 years old; TNM stage: I-IV; ICD-10: C34.1 and C34.3) were collected from Jinan Central Hospital Affiliated to Shandong University (Jinan, China) and stored immediately at -80˚C for subsequent analysis. Pathologists confirmed the correct identification of the tumour tissues and paired normal tissues. The present study was approved (approval no. W202203060147) by the Ethics Committee of Jinan Central Hospital Affiliated to Shandong First Medical University (Jinan, China). Written informed consent was obtained from all enrolled patients.

Cell culture and transfection. Normal human lung epithelial cells (BEAS-2B; cat. no. CRL-3588) and lung cancer cells [H1975 (cat. no. CRL-5908), H1688 (cat. no. CCL-257), H1299 (cat. no. CRL-5803) and A549 (cat. no. CRM-CCL-185)] were obtained from the American Type Culture Collection. Cells were maintained in Dulbecco's modified Eagle's medium (DMEM; Sigma-Aldrich; Merck KGaA) at 37˚C with 5% CO_2. Small interfering (si)RNAs si1-HSPB7 and si2-HSPB7, which specifically targeted HSPB7 were synthesized and purified by Guangzhou RiboBio Co., Ltd. The sequences were as follows: si1-HSPB7 sense, 5'-GGUGCUGUGGGAGGACAAAGA-3' and antisense, 5'-UUUGUCCUCCCACAGCACCUG-3'; si2-HSPB7 sense, 5'-GGAAGACUAUGUCACACUGCC-3', and antisense, 5'-CAGUGUGACAUAGUCUUCCUG-3'; si1-MECOM sense, 5'-GGAUGAUGAAGAAGUUGAAGA-3' and antisense, 5'-UUCAACUUCUUCAUCAUCCAG-3'; si2-MECOM sense, 5'-CCUGCUAGUUCUCCUGUUAAA-3' and antisense, 5,-UAACAGGAGAACUAGCAGGUA-3' and si-NC sense, 5'-UUCUCCGAACGUGUCACGUTT-3' and antisense, 5,'-ACGUGACACGUUCGGAGAATT-3'. HSPB7 and MECOM were cloned into the pcDNA3.1 eukaryotic expression vector to allow their overexpression. All the vectors were purchased from Guangzhou RiboBio Co., Ltd. When the fusion rate of H1975 and A549 cells reached 70-80%, Cells were transfected with 40 nM vectors using Lipofectamine 2000 reagent (Thermo Fisher Scientific, Inc.) for 10 h at 37˚C. After 48 h, the transfection efficiency was tested by quantitative reverse transcription-quantitative polymerase chain reaction (RT-qPCR). Before transfection, H1975 cells were pretreated with 5 mM 2-deoxy-D-glucose (2-DG; Sigma-Aldrich; Merck KGaA) for 8 h.

RT-qPCR. Total RNA was isolated from tissues and cells by homogenization using TRIzol® (Invitrogen; Thermo Fisher Scientific, Inc.). cDNA was synthesized using a PrimeScript RT Reagent kit (Takara Bio, Inc.) according to the manufacturer's protocols. The SYBR Green System (Takara Bio, Inc.) was used to assess gene expression. The sequences of primers used for amplification were as follows: HSPB7 forward, 5'-AACCACATCGAGCTGGCG-3' and reverse, 5'-GAAAGGGAAGGGAGAGGCAC-3'; MECOM forward, 5'-CTTCTTGACTAAAGCCCTTGGA-3' and reverse, 5'-GTACTTGAGCCAGCTTCCAACA-3'; and glyceraldehyde-3-phosphate dehydrogenase (GAPDH) forward, 5'-AATGGGCAGCCGTTAGGAAA-3' and reverse, 5'-GCCCAATACGACCAAATCAGAG-3'. The thermocycling conditions involved initial denaturation at 95˚C for 4 min; 40 cycles of denaturation at 95˚C for 15 sec, annealing at 60˚C for 35 sec, elongation at 72˚C for 30 sec; and final extension at 72˚C for 10 min. The $2^{-\Delta\Delta Cq}$ method (20) was used to calculate the mRNA expression level. Expression levels were normalized to the internal reference gene, GAPDH.

Western blotting. Total protein from the cells was isolated and quantified using radioimmunoprecipitation (RIPA) assay lysis buffer and a bicinchoninic acid kit (both from Beyotime Institute of Biotechnology), respectively. Samples (30 μg) were separated by 12% polyacrylamide gel electrophoresis and transferred onto polyvinylidene fluoride (PVDF) membranes. After blocking with 5% skim milk for 1 h at room temperature, the membranes were incubated overnight at 4˚C with the following primary antibodies: HSPB7 monoclonal antibody (1:1,000; cat. no. ab248960; Abcam), E-cadherin polyclonal antibody (1:1,000; cat. no. GB11868; Wuhan Servicebio Technology Co., Ltd.), N-cadherin polyclonal antibody (1:1,000; cat. no. GB111009; Wuhan Servicebio Technology Co., Ltd.), Snail polyclonal antibody (1:1,000; cat. no. 13099-1-AP; Proteintech Group, Inc.), lactate dehydrogenase A (LDHA) polyclonal antibody (1:1,000; cat. no. 19987-1-AP; Proteintech Group,

Table I. Clinical characteristics of the lung adenocarcinoma patients from The Cancer Genome Atlas.

Clinical characteristics	Number	Percentage, %
Age, years		
<65	239	46.4
≥65	276	53.6
Sex		
Female	277	53.8
Male	238	46.2
Stage		
I	275	53.4
II	122	23.7
III	73	14.2
IV	11	2.1
T classification		
T1	169	32.8
T2	277	53.8
T3	47	9.1
T4	19	3.7
TX	3	0.6
M classification		
M0	346	67.2
M1	25	4.9
MX	140	27.2
Missing data	4	0.8
N classification		
N0	331	64.3
N1	96	18.6
N2	74	14.4
N3	2	0.4
NX	11	2.1
Missing data	1	0.2
ICD-10		
C34.0	2	0.4
C34.1	310	60.2
C34.2	20	3.9
C34.3	174	33.8
C34.8	4	0.8
C34.9	5	1.0

ICD, International Classification of Diseases.

Table II. Clinical characteristics of the lung adenocarcinoma patients from our hospital.

Clinical characteristics	Number	Percentage, %
Age, years		
<65	9	39.1
≥65	14	60.9
Sex		
Female	10	43.5
Male	13	56.5
Stage		
I	8	34.8
II	11	47.8
III	3	13.0
IV	1	4.3
T classification		
T1	7	30.4
T2	13	56.5
T3	2	8.7
T4	1	4.3
M classification		
M0	20	87.0
M1	3	13.0
N classification		
N0	19	82.6
N1	3	13.0
N2	1	4.3
ICD-10		
C34.1	15	65.2
C34.3	8	34.8

ICD, International Classification of Diseases.

Inc.), hexokinase 2 (HK2) monoclonal antibody (1:1,000; cat. no. 2867; Cell Signaling Technology, Inc.); pyruvate kinase muscle isoform 2 (PKM2) polyclonal antibody (1:500; cat. no. SAB4200094; Sigma-Aldrich; Merck KGaA) and GAPDH polyclonal antibody (1:1,000; cat. no. AC001; ABclonal Biotech Co., Ltd.). The PVDF membranes were then incubated with the HRP-conjugated secondary antibody goat anti-rabbit IgG (1:5,000; cat. no. AS014; ABclonal Biotech Co., Ltd.) at room temperature for 1 h. The bands were visualized using enhanced chemiluminescence (Beijing Solarbio Science & Technology Co., Ltd.) and quantified using Quantity One® 4.1.1 gel analysis software (Bio-Rad Laboratories, Inc.). GAPDH was used as the loading control.

Immunohistochemistry (IHC) analysis. The lung tissue and xenograft tumours sections were deparaffinized with xylene and rehydrated in gradient ethanol at room temperature. To eliminate endogenous peroxidase activity, the sections (4 μm) were incubated with 3% H_2O_2 at room temperature for 5-10 min. Subsequently, the sections were rinsed three times with distilled water and soaked in phosphate buffered saline for 5 min. After blocking in 5-10% normal goat serum (cat. no. SL038; Beijing Solarbio Science & Technology Co., Ltd.) for 10 min, the sections were incubated with primary antibodies against HSPB7 (1:200; cat. no. ab150390; Abcam) and Ki67 (1:200; cat. no. ab15580; Abcam) overnight at 4˚C, followed by HRP-conjugated secondary antibody (1:200) at 37˚C for 1 h. Finally, the sections were stained with the developer 3,3'-diaminobenzidine (Beijing Solarbio Science & Technology Co., Ltd.) for 3-15 min and observed under a light microscope (DMI3000 B; Leica Microsystems GmbH).

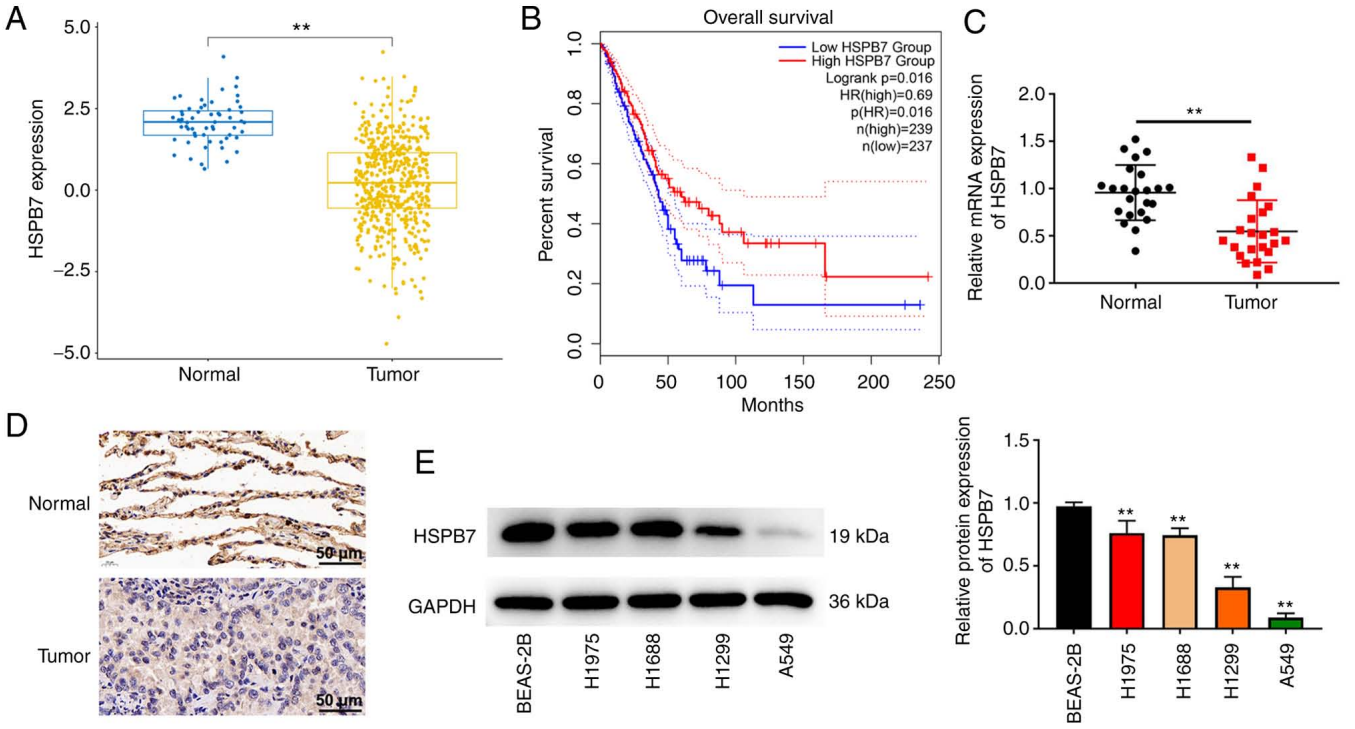

Figure 1. HSPB7 is downregulated in LUAD tissues and cells. (A) HSPB7 expression in the TCGA-LUAD cohort datasets was analysed. **P<0.01 by unpaired Student's t-test. (B) Kaplan-Meier survival analysis based on TCGA-LUAD datasets was analysed. (C) The expression of HSPB7 in 23 cases of LUAD tumour and paired normal tissues was determined through reverse transcription-quantitative PCR. Data are shown as the mean ± SD (n=3). **P<0.01 by paired Student's t-test. (D) The protein expression of HSPB7 in tumour and paired normal tissues of LUAD patients was detected by immunohistochemistry. (E) The protein expression of HSPB7 in human normal lung epithelial cells (BEAS-2B) and lung cancer cells (H1975, H1688, H1299 and A549) was detected by western blotting. Data are presented as the mean ± SD (n=3). **P<0.01 vs. BEAS-2B by one-way ANOVA test, followed by Tukey's post hoc test. HSPB7, heat shock protein B7; LUAD, lung adenocarcinoma; TCGA, The Cancer Genome Atlas.

3-(4,5-dimethylthiazol-2-yl)-2,5-diphenyl-2-Htetrazolium bromide (MTT) assay. After transfection, H1975 and A549 cells ($1x10^3$ cells/well) were seeded into a 96-well plate and cultured at 37˚C for 24, 48 and 72 h. Next, cells were treated with 10 μl MTT reagent (Beyotime Institute of Biotechnology) at 37˚C for 4 h, dimethyl sulfoxide (Thermo Fisher Scientific, Inc.) was applied to treat cells at room temperature for 10 min, and the value of optical density was measured at 570 nm using a microplate reader (BioTek Instruments, Inc.).

Colony formation. After transfection, H1975 and A549 cells ($5x10^2$ cells/well) were seeded into six-well plates. After ~14 d, visible clones appeared in the six-well plates. Colonies (>50 cells) were fixed with 4% formaldehyde for 15 min and stained with 0.1% crystal violet (both from Sigma-Aldrich; Merck KGaA) for 25 min. Finally, the number of effective clones was calculated using a microscope (DMI3000 B; Leica Microsystems GmbH).

Wound healing assay. H1975 and A549 cells ($4x10^5$ cells/well) were seeded in six-well cell culture plates. When the confluence of the monolayer cells reached 70-80%, a new 200-μl pipette tip was used to gently scratch a wound on the monolayer cells. Cells were cultured in serum-free medium for 48 h. Images were captured by a microscope (DMI3000 B; Leica Microsystems GmbH) at 0 and 48 h, and the wound width was analyzed using ImageJ software v1.51 (National Institutes of Health).

Transwell assay. A 6.5 mm Transwell with 8.0 μm Pore Polycarbonate Membrane Insert, Sterile (Corning, Inc.) was used in invasion assay. The transfected H1975 and A549 cells ($1x10^5$ cells/ml) were resuspended in serum-free DMEM in the upper chamber with Matrigel (BD Biosciences) at 37˚C for 30 min, while the lower chamber was filled with 150 μl DMEM containing 10% fetal bovine serum (Gibco; Thermo Fisher Scientific, Inc.). After culturing at 37˚C for 48 h, 800 μl methanol and 800 μl crystal violet were used to fix for 15 min at room temperature and stain for 30 min at room temperature cells. A total of five randomly selected fields were observed under microscope (Leica Microsystems GmbH).

Glucose and lactate measurement. A Glucose Assay kit (cat. no. ab65333; Abcam) and a Lactic Acid Assay kit (cat. no. MAK064, Sigma-Aldrich; Merck KGaA) were used to measure glucose consumption and lactic acid production, respectively, in H1975 and A549 cells. Glucose enzyme mix specifically oxidizes glucose, to generate a product which reacts with a dye to generate color (OD 570 nm). Glucose content in the cell culture medium was determined and cells in each well were counted to normalize glucose concentration. Glucose uptake was determined indirectly by determining the remained glucose content in cell culture medium. Lactate specifically reacts with an enzyme mix to generate a product, which interacts with lactate probe to produce color (OD 570 nm). Lactate production in the cell culture medium was detected and cells in each well were

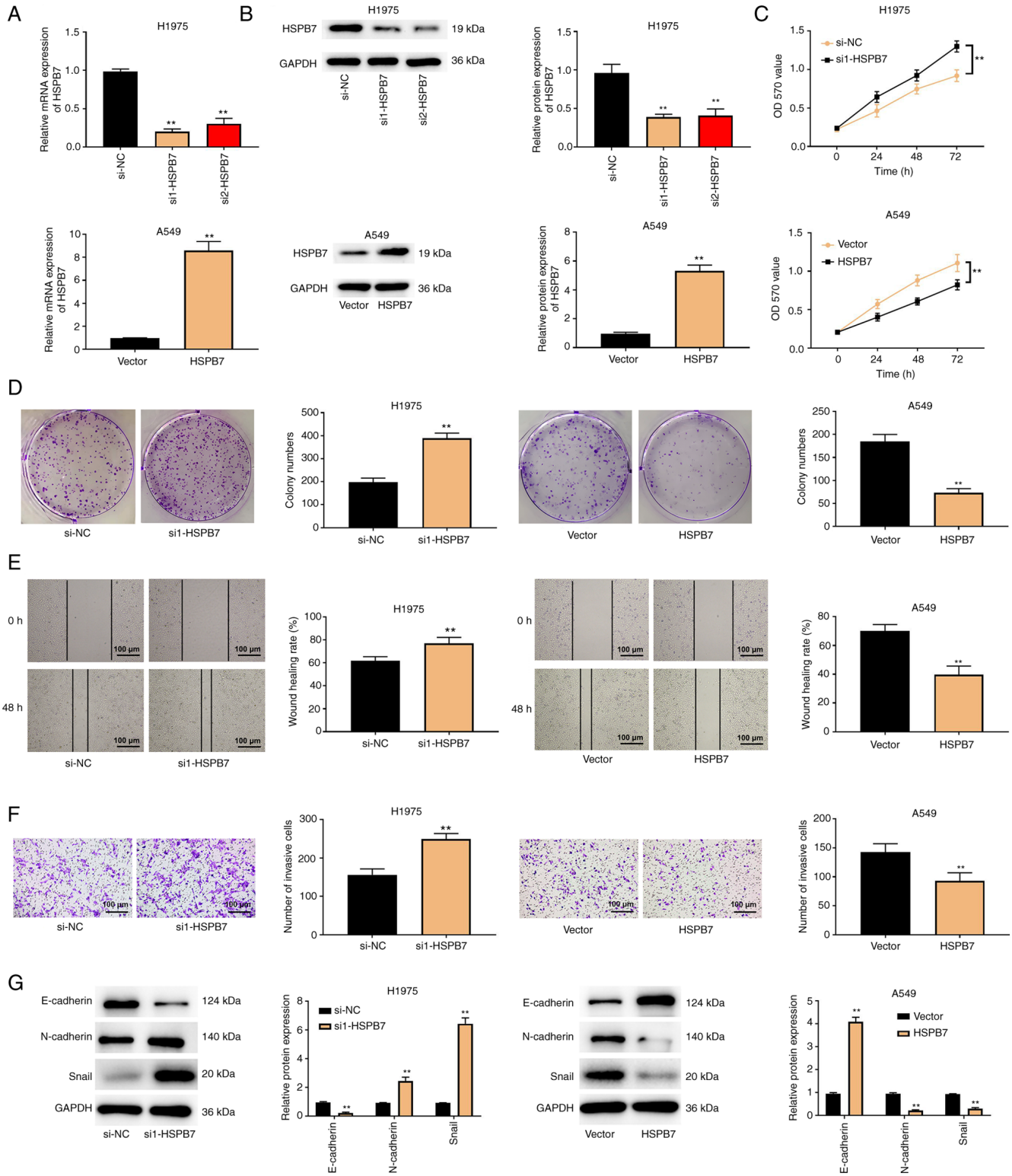

Figure 2. HSPB7 restricts lung adenocarcinoma cell proliferation, migration, invasion and EMT. (A) The H1975 and A549 cells were transfected with si-NC, si1-HSPB7, si2-HSPB7, vector, and HSPB7. HSPB7 expression in H1975 and A549 cells was determined through reverse transcription-quantitative PCR. (B) HSPB7 protein expression in H1975 and A549 cells was measured using western blotting. The H1975 and A549 cells were transfected with si-NC, si1-HSPB7, vector and HSPB7. (C) MTT assay, (D) colony formation assay, (E) wound healing assay and (F) Transwell assay were used to evaluate H1975 and A549 cell proliferation, migration and invasion. (G) EMT-related proteins, including E-cadherin, N-cadherin and Snail were detected in H1975 and A549 cells via western blotting. Data are shown as the mean ± SD (n=3). **P<0.01 vs. si-NC or vector group by unpaired Student's t test. HSPB7, heat shock protein B7; EMT, epithelial-mesenchymal transition; si-, small interfering; NC, negative control.

counted to normalize lactate concentration. Absorbance at OD 570 nm was detected using a microplate reader (BioTek Instruments, Inc.).

Co-Immunoprecipitation (Co-IP). Whole-cell extracts were lysed in RIPA buffer (Beyotime Institute of Biotechnology). Lysates were clarified by centrifugation at 14,000 g for 15 min

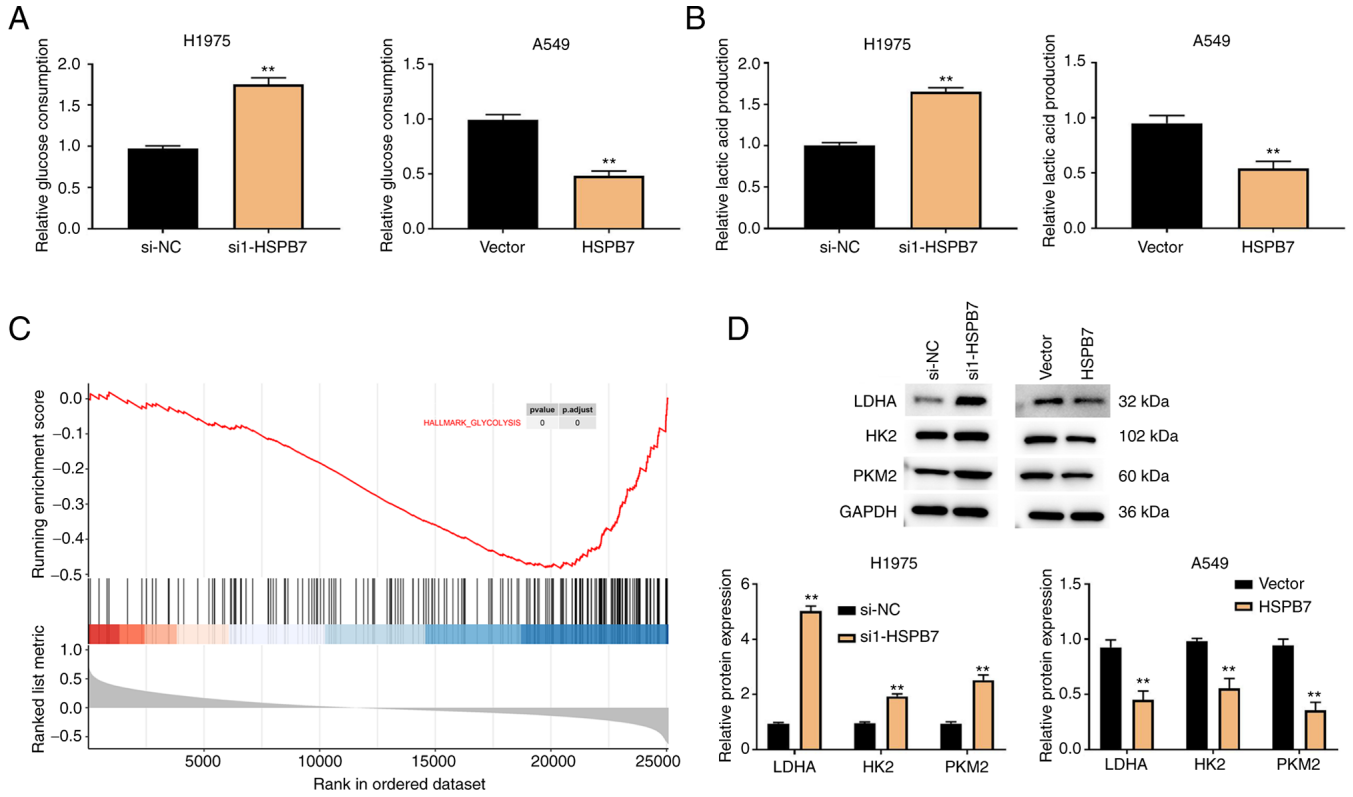

Figure 3. HSPB7 inhibits glycolysis. The H1975 and A549 cells were transfected with si-NC, si1-HSPB7, vector and HSPB7. (A) Glucose consumption in H1975 and A549 cells was detected using Glucose Assay kit. (B) Lactic acid production in H1975 and A549 cells was evaluated using Lactic Acid Assay kit. (C) Gene set enrichment analysis showed that HSPB7 could inhibit glycolysis. (D) Western blotting was used to detect glycolysis-associated proteins (PKM2, LDHA and HK2) in H1975 and A549 cells. Data are shown as the mean ± SD (n=3). **P<0.01 vs. si-NC or vector group by unpaired Student's t test. HSPB7, heat shock protein B7; si-, small interfering; NC, negative control; PKM2, pyruvate kinase muscle isoform 2; LDHA, lactate dehydrogenase A; HK2, hexokinase 2.

at 4˚C. Supernatant was incubated with 20 μl/ml protein A/G sepharose beads (Beyotime Institute of Biotechnology) at 4˚C for 1 h to remove non-specific hybrid proteins. A total of 5 μg IgG (cat. no. ab37415; Abcam), anti-HSPB7 (cat. no. ab150390; Abcam) or anti-MECOM (cat. no. 23201-1-AP; Proteintech Group, Inc.) antibodies were added to pre-cleared cell lysate and incubated at 4˚C overnight and then rotated at 4˚C with a mixture of protein A/G sepharose beads (20 μl/ml) for 4 h. The beads were then washed 3 times with RIPA buffer to obtain protein samples for western blot analysis.

Chromatin immunoprecipitation (ChIP). In brief, H1975 and A549 cells were first cross-linked with formaldehyde at room temperature for 15 min, and then cleaved by the Magna ChIP™ Protein G Kit (Sigma-Aldrich; Merck KGaA) to obtain chromatin, followed by ultrasonic fragmentation. MECOM antibody (cat. no. HPA046537; Sigma-Aldrich; Merck KGaA) was used to recruit HSPB7 DNA overnight at 4˚C, and the protein-DNA complex was precipitated with protein G magnetic beads for 2 h. After immunoprecipitation, the DNA in the complex was purified, and enriched HSPB7 was quantified by PCR.

Tumorigenesis assay. Male nude mice aged 4-6 weeks (weight, 14-15 g; GemPharmatech Biotechnology Co., Ltd.) were used, with five mice per experimental group. All mice were maintained under controlled temperature (22±1˚C) and humidity (50±5%) in a 12/12-h light/dark cycle with food and water available *ad libitum*. A total of $1x10^6$ control cells and A549 cells with overexpression of HSPB7 were resuspended in phosphate-buffered saline and injected subcutaneously into the back flank of mice, and tumour volume was recorded every 3 days. Tumor volume >2,000 mm^3 was considered the humane endpoint. The tumor volume was calculated as follows: Volume=0.5x length x $width^2$. At the end of the experiments, the weight of the mice was 18-19 g. After 27 days, mice were sacrificed by cervical dislocation under anesthesia (pentobarbital sodium, 50 mg/kg, intraperitoneal injection) and confirmed the sacrifice by cessation of heartbeat. Animal experiments were approved (approval no. W202203060148) by the Animal Ethics Committee of Jinan Central Hospital Affiliated to Shandong First Medical University (Jinan, China).

Statistical analysis. All statistical analyses were performed using GraphPad Prism 6 software (Dotmatics). All data are presented as the mean ± SD. Each experiment was performed in triplicate. Survival curves were analysed by the Kaplan-Meier method and compared by the log-rank test. Comparisons were analysed using the paired or unpaired Student's t-test or one-way ANOVA, followed by Tukey's post hoc test. Pearson's correlation analysis was performed to assess the correlation between MECOM and HSPB7 expression levels in the tumour tissues. P<0.05 was considered to indicate a statistically significant difference.

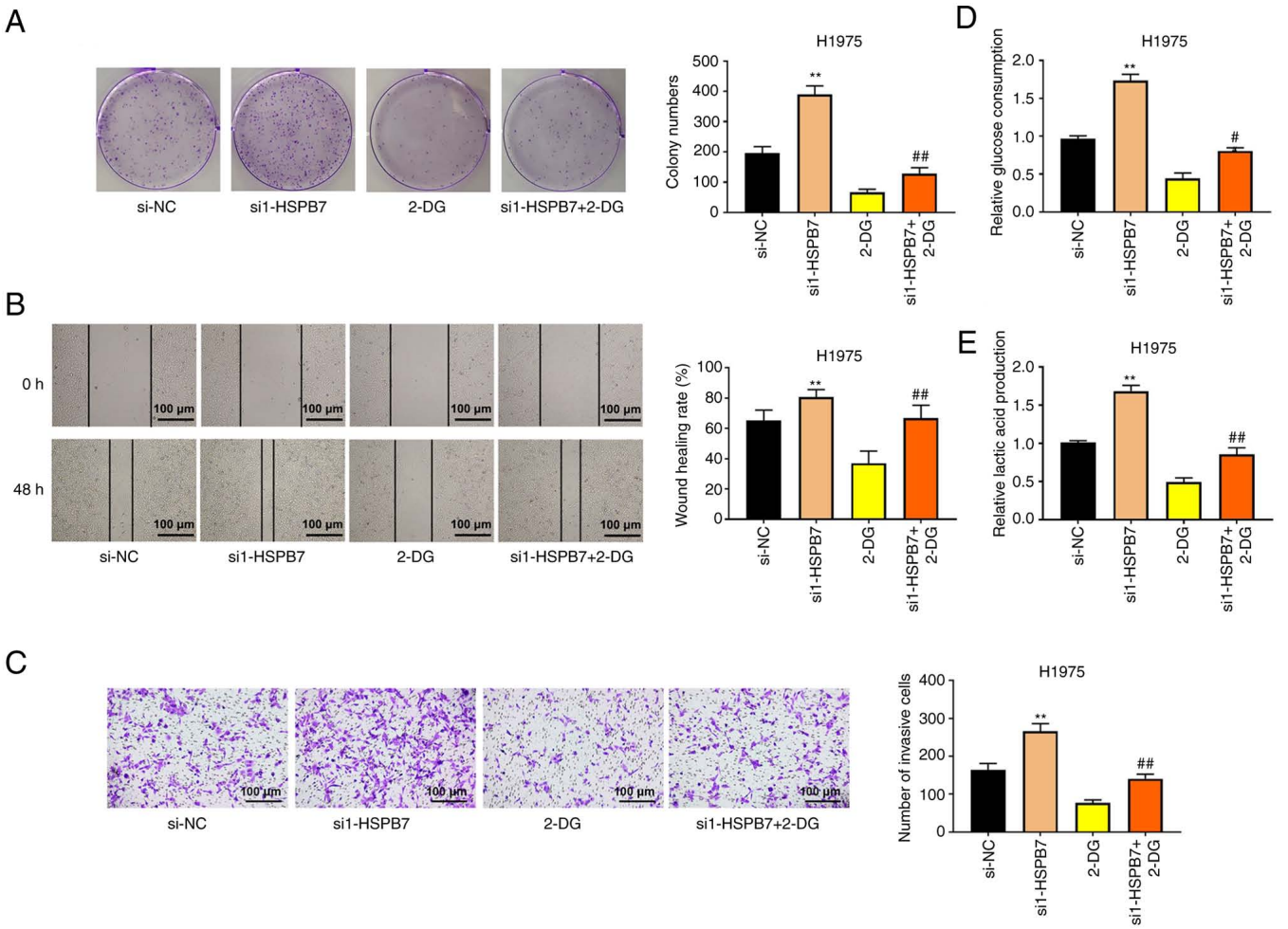

Figure 4. Silencing HSPB7 promotes the proliferation, migration, and invasion of lung adenocarcinoma cells by regulating glycolysis. The H1975 cells were transfected with si-NC or si1-HSPB7, followed by treating with or without glycolysis inhibitor 2-DG. (A) Colony formation assay, (B) wound healing assay and (C) Transwell assay were used to evaluate H1975 cell proliferation, migration and invasion. (D) Glucose consumption in H1975 cells was detected using Glucose Assay kit. (E) Lactic acid production in H1975 cells was evaluated using Lactic Acid Assay kit. Data are shown as the mean ± SD (n=3). **P<0.01 vs. si-NC group; $^{\#}$P<0.05 vs. si1-HSPB7 group; $^{\#\#}$P<0.01 vs. si1-HSPB7 group by one-way ANOVA test, followed by Tukey's post hoc test. HSPB7, heat shock protein B7; si-, small interfering; NC, negative control; 2-DG, 2-deoxy-D-glucose.

Results

HSPB7 expression is downregulated in LUAD tissues and cells. A total of 515 patients with LUAD were acquired from TCGA-LUAD cohort datasets and analyzed to identify the HSPB7 expression in LUAD. The detailed clinical features of the patients are listed in Table I. As revealed in Fig. 1A, HSPB7 expression was downregulated in LUAD tumour tissues compared with non-tumour tissues. Survival analysis demonstrated that patients with high HSPB7 expression had a higher survival rates (Fig. 1B). The detailed clinical features of the 23 tumor tissues and paired normal tissues are presented in Table II. The RT-qPCR and IHC data indicated that HSPB7 was expressed at low levels in LUAD tumour tissues compared with the paired normal tissues (Fig. 1C and D). In addition, the expression of HSPB7 protein was detected in lung cancer cell lines. HSPB7 expression showed different degrees of reduction in the H1975, H1688, H1299 and A549 cells compared with that in BEAS-2B cells (Fig. 1E). To further clarify the role of HSPB7 in LUAD, H1975 cells with the highest HSPB7 expression and A549 cells with the lowest expression were selected among the four cell lines for a follow-up study.

HSPB7 restricts LUAD cell proliferation, migration, invasion and epithelial-mesenchymal transition (EMT). To improve understanding of the effects of HSPB7 on LUAD cell behaviour, cell proliferation, migration, invasion and EMT were evaluated. First, HSPB7 low expressing and overexpressing cells were constructed, and RT-qPCR and western blotting results revealed that the construction was successful (Fig. 2A and B). In the MTT and colony formation assays, it was observed that knockdown of HSPB7 promoted H1975 cell proliferation, while overexpression of HSPB7 inhibited A549 cell proliferation (Fig. 2C and D). In wound healing and Transwell experiments, the data also revealed that low expression of HSPB7 promoted H1975 cell migration and invasion, whereas overexpression of HSPB7 inhibited A549 cell migration and invasion (Fig. 2E and F). As western blotting results demonstrated, HSPB7 knockdown significantly reduced E-cadherin protein expression and increased the protein expression of N-cadherin and Snail in H1975 cells.

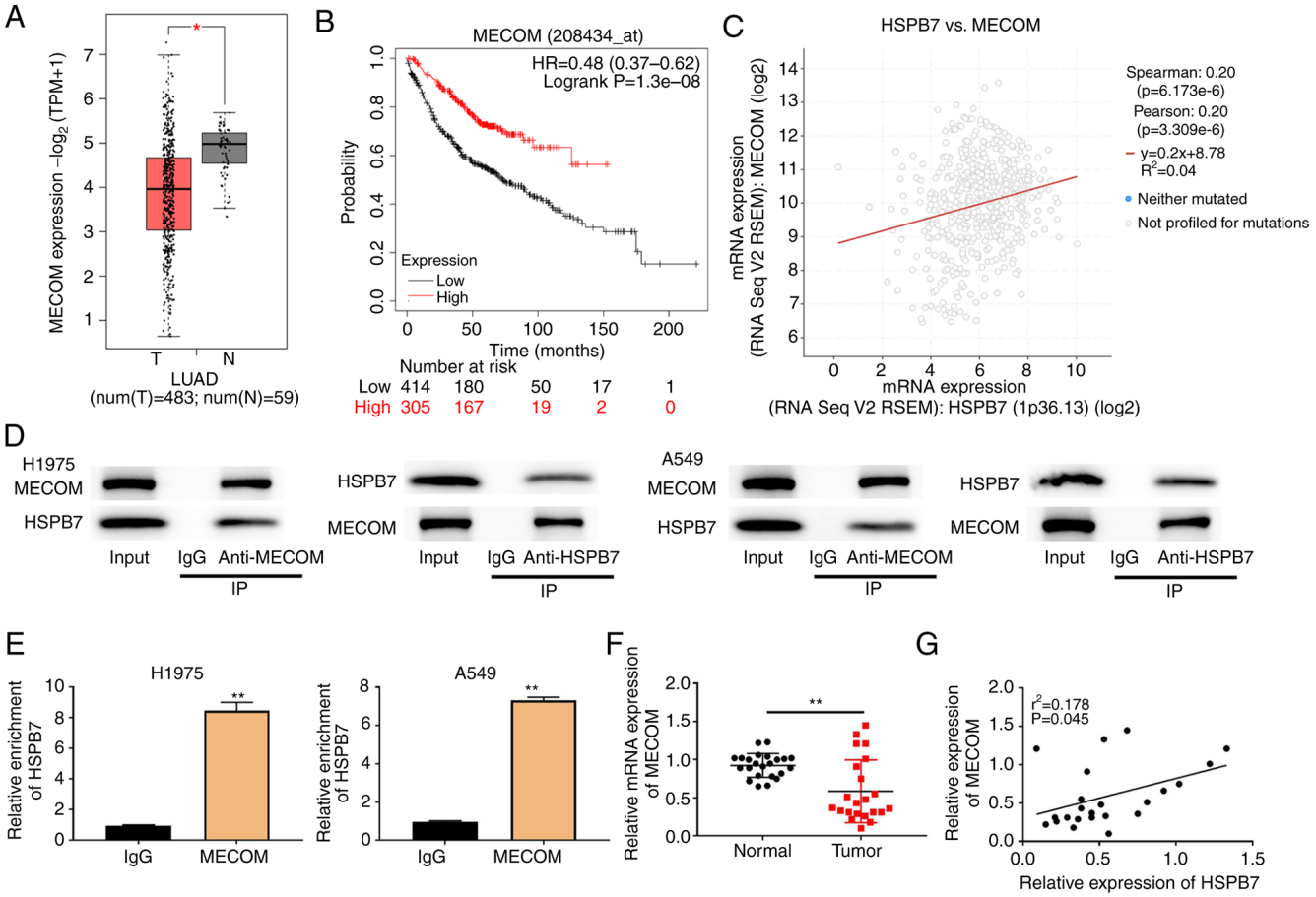

Figure 5. MECOM is transcription factor of HSPB7. (A) MECOM expression in the TCGA-LUAD cohort datasets was analysed. (B) Kaplan-Meier survival analysis based on TCGA-LUAD datasets was analysed. (C) Correlation analysis between MECOM and HSPB7 based on TCGA-LUAD datasets using Pearson's correlation analysis. (D) Co-IP confirmed the binding between HSPB7 and MECOM in H1975 and A549 cells (E) Chromatin Immunoprecipitation assay was used to verify the binding ability of HSPB7 to transcription factor MECOM; Data are shown as mean ± SD (n=3). **P<0.01 vs. lgG group by unpaired Student's t-test. (F) The expression of MECOM in twenty-three cases of LUAD tumour and paired normal tissues was detected by reverse transcription-quantitative PCR; Data are presented as the mean ± SD (n=3). **P<0.01 by paired Student's t-test. (G) Correlation analysis of MECOM and HSPB7 in LUAD tumour tissues using Pearson's correlation analysis. **P<0.01 by paired Student's t-test. MECOM, myelodysplastic syndrome 1 and ecotropic viral integration site 1 complex locus; HSPB7, heat shock protein B7; TCGA, The Cancer Genome Atlas; LUAD, lung adenocarcinoma; Co-IP, Co-Immunoprecipitation; HR, hazard ratio.

Conversely, overexpression of HSPB7 increased the expression of E-cadherin protein and inhibited the protein expression of N-cadherin and Snail in A549 cells (Fig. 2G).

HSPB7 inhibits glycolysis. To support uncontrolled proliferation, migration and invasion, LUAD cells can shift their glucose metabolism pattern to aerobic glycolysis (21). It was hypothesized that HSPB7 participates in the regulation of aerobic glycolysis, thereby affecting LUAD progression. As revealed in Fig. 3A and B, low HSPB7 expression increased glucose consumption and lactic acid production in H1975 cells. On the contrary, when HSPB7 was overexpressed, A549 cells reduced glucose consumption and lactic acid production. Furthermore, GSEA revealed that HSPB7 was involved in glycolysis in LUAD cells (Fig. 3C). Therefore, it was hypothesized that HSPB7 participates in the regulation of LUAD by inhibition of glycolysis. To test this hypothesis, the levels of the glycolysis-associated proteins (LDHA, HK2 and PKM2) were examined in the H1975 and A549 cells. The results of western blotting indicated that HSPB7 knockdown increased the expression of LDHA, HK2 and PKM2, whereas HSPB7 overexpression inhibited the expression of LDHA, HK2 and PKM2 (Fig. 3D).

HSPB7 inhibits the proliferation, migration, and invasion of LUAD cells by regulating glycolysis. To analyze the relationship among HSPB7, glycolysis and tumour progression, the glycolysis inhibitor, 2-DG, was added into the H1975 cells that silenced HSPB7 expression. 2-DG is a glucose analogue that differs from glucose only by the removal of an oxygen atom at the C-2 position, which prevents the isomerization of glucose-6-phosphate to fructose-6-phosphate, thereby inhibiting glycolysis (22). As shown in Fig. 4A, silencing of HSPB7 promoted H1975 proliferation, but the addition of 2-DG weakened the promoting effect of si1-HSPB7 on cell proliferation. The cell migration and invasion abilities were significantly reduced in the si1-HSPB7 + 2-DG group compared with si1-HSPB7 group (Fig. 4B and C). In addition, it was observed that 2-DG significantly reduced the consumption of glucose and production of lactic acid induced by HSPB7 knockdown in H1975 cells (Fig. 4D and E).

MECOM is a transcription factor of HSPB7. TCGA dataset analysis identified that MECOM was poorly expressed in LUAD tumour tissues, and the survival rate of patients

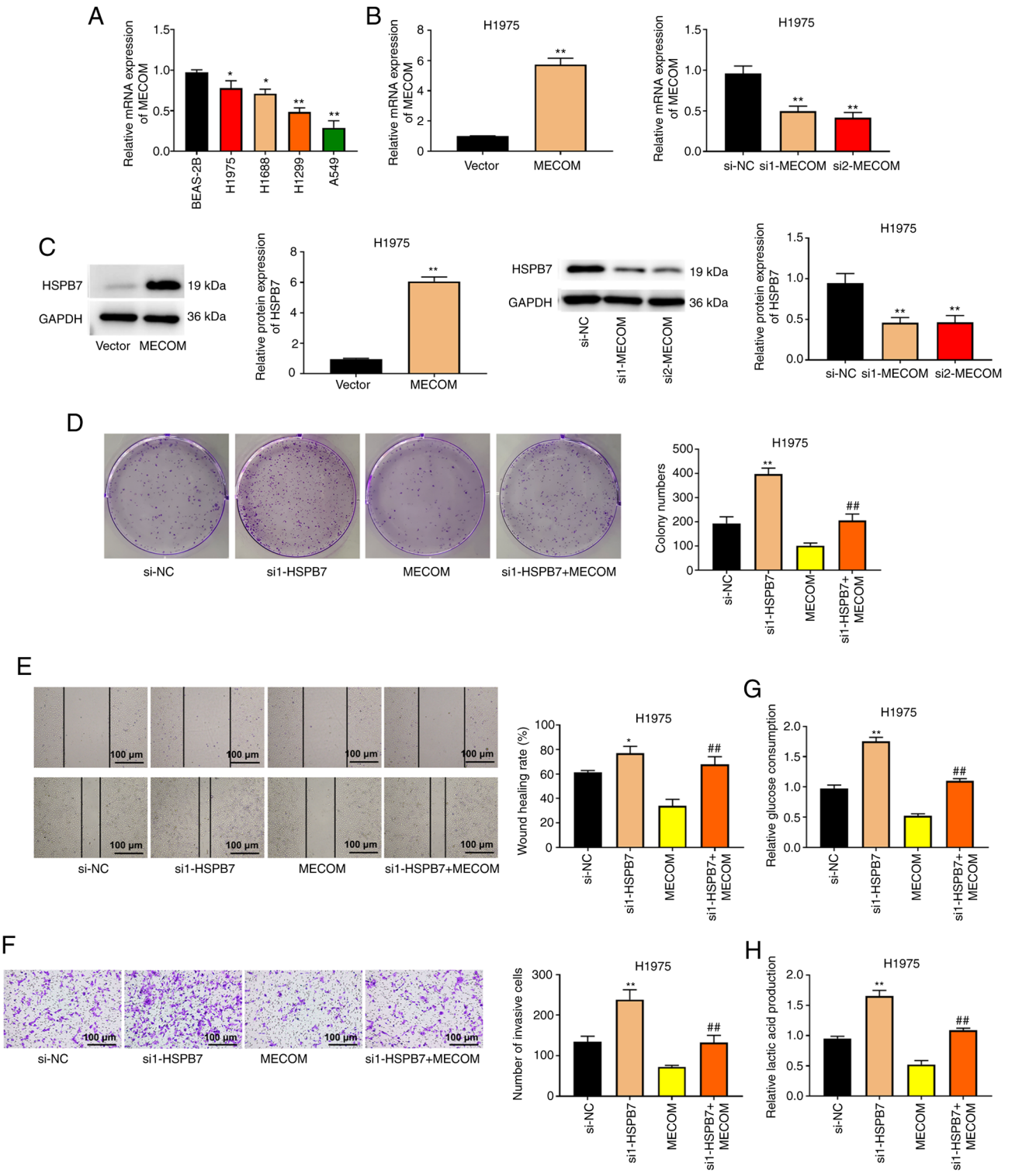

Figure 6. HSPB7 is regulated by the transcription factor MECOM. (A) The mRNA expression of MECOM in human normal lung epithelial cells (BEAS-2B) and lung cancer cells (H1975, H1688, H1299 and A549) was detected using RT-qPCR. The H1975 cells were transfected with si-NC, si1-HSPB7, MECOM, si1-MECOM, or si2-MECOM. (B) The mRNA expression of MECOM in H1975 cells was measured using RT-qPCR. (C) HSPB7 protein expression in H1975 cells was measured using western blot analysis. (D) Colony formation assay, (E) wound healing assay and (F) Transwell assay were respectively to evaluate H1975 cell proliferation, migration and invasion. (G) Glucose consumption in H1975 cells was detected using Glucose Assay kit. (H) Lactic acid production in H1975 cells was evaluated using Lactic Acid Assay kit. Data are shown as the mean ± SD (n=3). *P<0.05 vs. BEAS-2B or si-NC group; **P<0.01 vs. BEAS-2B, si-NC, or vector group; $^{\#\#}$P<0.01 vs. MECOM group by one-way ANOVA test with Tukey's post hoc test. HSPB7, heat shock protein B7; MECOM, myelodysplastic syndrome 1 and ecotropic viral integration site 1 complex locus; RT-qPCR, reverse transcription-quantitative PCR; si-, small interfering; NC, negative control.

with low MECOM expression was also relatively low (Fig. 5A and B). Furthermore, MECOM levels were positively correlated with HSPB7 expression (Fig. 5C). Co-IP assays were conducted in H1975 and A549 cells. The results of Co-IP revealed that HSPB7 could interact with MECOM (Fig. 5D). According to JASPAR website analysis, the

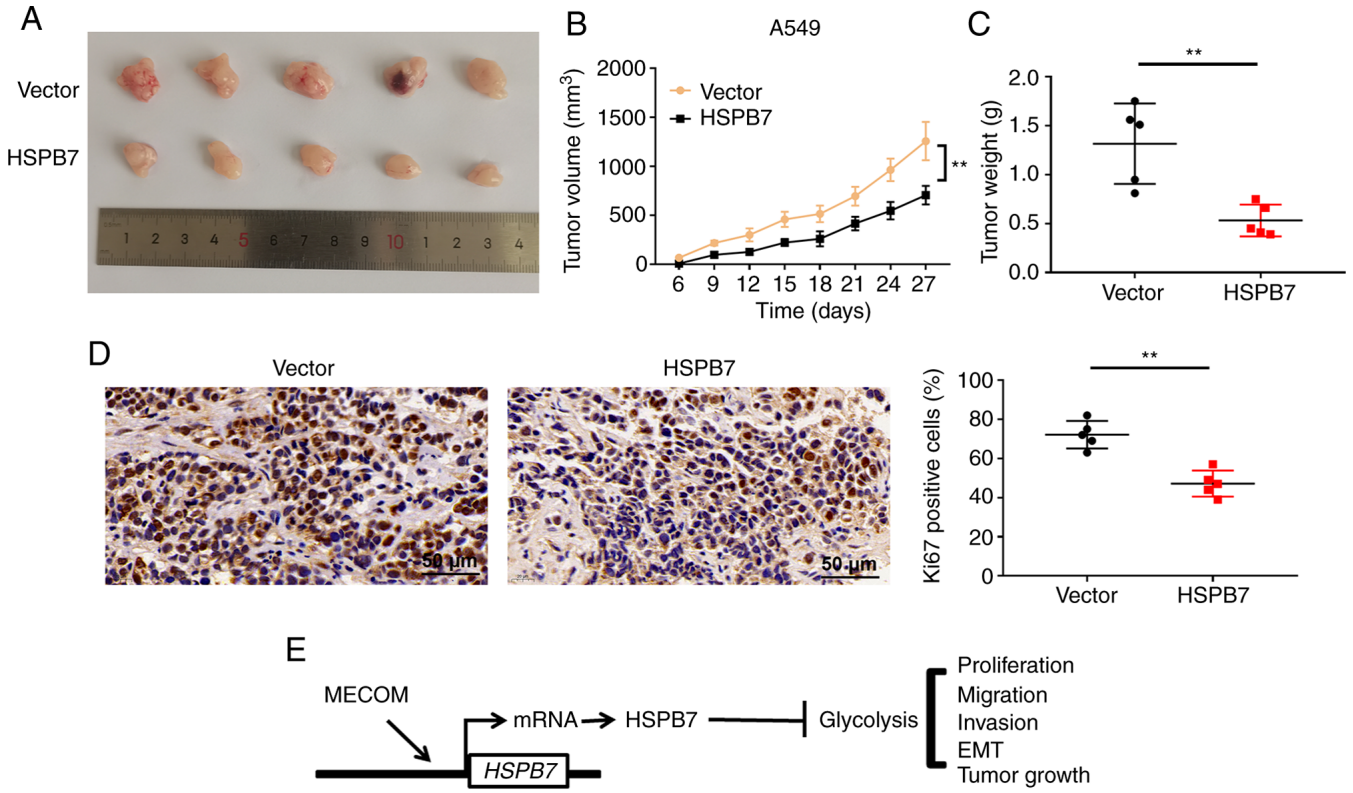

Figure 7. HSPB7 suppresses tumour growth. (A) Representative image of tumour xenografts harvested at day 27. (B) Tumour growth curves from the two groups. (C) Tumour weights from the two groups. (D) The Ki67 positive cell in the two groups was detected by immunohistochemistry. (E) A schematic diagram of HSPB7 hindering lung adenocarcinoma progression through inhibition of glycolysis. Data are presented as the mean ± SD (n=5). **P<0.01 by unpaired Student's t-test. HSPB7, heat shock protein B7; MECOM, myelodysplastic syndrome 1 and ecotropic viral integration site 1 complex locus; EMT, epithelial-mesenchymal transition.

binding site of MECOM is located within 1 kb upstream of HSPB7. To verify this, ChIP analysis was performed and it was found that HSPB7 was significantly enriched in the MECOM group (Fig. 5E). The RT-qPCR results revealed that MECOM was downregulated in tumour tissues, and there was a positive correlation between the levels of MECOM and HSPB7 (Fig. 5F and G).

HSPB7 is regulated by the transcription factor MECOM. The expression levels of MECOM mRNA in the lung cancer cell lines were also measured. MECOM mRNA expression was decreased in H1975, H1688, H1299 and A549 cells compared with BEAS-2B cells (Fig. 6A). To clarify the roles of HSPB7 and MECOM in LUAD, rescue experiments were conducted in H1975 cells. As demonstrated in Fig. 6B, MECOM expression was increased in H1975 cells transfected with MECOM overexpression plasmid, whereas was decreased in H1975 cells transfected with si-MECOM. Overexpression of MECOM increased HSPB7 protein expression, while silencing of MECOM decreased HSPB7 protein expression (Fig. 6C). In terms of proliferation, overexpression of MECOM decreased the colony number of H1975 cells, but co-transfection of si1-HSPB7 reversed the inhibitory effect of MECOM on cell proliferation (Fig. 6D). The migration and invasion abilities of H1975 cells in the si1-HSPB7 + MECOM group were significantly higher than those in the MECOM group (Fig. 6E and F). In addition, the consumption of glucose and production of lactic acid by the H1975 cells in the si1-HSPB7+MECOM group were increased compared with MECOM group (Fig. 6G and H).

HSPB7 suppresses tumour growth. The effects of HSPB7 overexpression on the tumorigenic ability of A549 cells derived from nude mice were determined. Tumours derived from injected HSPB7 overexpression cells were significantly smaller than those derived from vector-transfected mice (Fig. 7A and B). The average weight of tumours from nude mice injected with HSPB7 overexpression cells was lower than that of tumours from nude mice injected with control A549 cells (Fig. 7C). The number of Ki67 positive cells, a marker of proliferation, in the HSPB7 overexpression group decreased significantly (Fig. 7D). These results suggested that overexpression of HSPB7 in A549 cells inhibited their tumorigenic ability.

Discussion

In the present study, the influence and underlying molecular mechanisms of HSPB7 on the biological behaviour of lung cancer cells were investigated. The present findings revealed that HSPB7 expression was downregulated in LUAD tissues and cells. MECOM was a transcription factor of HSPB7. Knockdown of HSPB7 promoted lung cancer cell proliferation, migration and invasion; all of which were related to glycolysis (Fig. 7E).

Late diagnosis and complex clinical features lead to poor prognosis in LUAD (23,24). Precision medicine

targeting the epidermal growth factor receptor, anaplastic lymphoma kinase, and ROS proto-oncogene 1, receptor tyrosine kinase (ROS1) has contributed significantly to the effective treatment of LUAD (25,26). Although targeted therapy has made some progress, an increasing number of specific molecular biomarkers and therapeutic targets are required to guide and improve the prognosis and treatment of LUAD. A previous study reported that HSPB7 expression is downregulated by methylation and that HSPB7 acts as a tumour suppressor regulated by p53 in renal cell carcinoma (17). In the present study, it was found that HSPB7 was significantly downregulated in LUAD tissues and cells, and that its aberrant expression correlated with survival in patients with LUAD. In addition, silencing of HSPB7 promoted LUAD cell proliferation, invasion and migration. HSPB7 acted as a tumour suppressor regulated by MECOM in LUAD. Naderi (16) confirmed that knockdown of HSPB7 promotes the proliferation of human breast cancer cells. EMT is closely related to primary invasion and secondary metastasis of a variety of tumours and its inhibition could prevent cancer progression (27). E-cadherin transforms into N-cadherin during EMT, and expression of E-cadherin, an epithelial cell marker, is downregulated (28). The E-cadherin suppressor, Snail, facilitates cancer cell migration and invasion (29). In the present study, silencing of HSPB7 promoted EMT in LUAD cells, which showed a decrease in E-cadherin protein and an increase in N-cadherin and Snail proteins; whereas, overexpression of HSPB7 led to the opposite findings. Taken together, these results suggested that HSPB7 plays a role in LUAD progression.

Increasing evidence has indicated that glycolysis promotes cancer progression (30,31). Therefore, it is a new strategy to delay tumor progression by inhibiting glycolysis in cancer cells. In cancer cells, elevated glycolysis promotes glucose uptake and lactic acid production to meet metabolic needs, thereby increasing cell proliferation and metastasis (7). Zhou *et al* (31) demonstrated that silencing of circRNA enolase 1 inhibits glucose uptake and lactic acid production, thereby inhibiting glycolysis and ultimately LUAD progression. Consistently, the present data demonstrated that HSPB7 reduced glucose consumption and lactic acid production in LUAD cells. In addition, the inhibition of glycolysis by 2-DG weakened the promoting effect of knockdown of HSPB7 on cell proliferation, migration and invasion. LDHA, HK2 and PKM2 are important factors in glycolysis and their overexpression is associated with poor prognosis of patients with lung cancer (32,33). The present study demonstrated that HSPB7 inhibits the expression of LDHA, HK2 and PKM2 in lung cancer cells. Collectively, HSPB7 inhibited the proliferation, migration and invasion of LUAD cells, all of which are related to glycolysis.

MECOM, also known as MDS1/EVI1, is located on chromosome 3q26.2. It encodes the MDS1 and EVI1 complex locus proteins and consists of 1051 amino acids (34). MECOM encodes zinc-finger transcription factors and participates in a series of biological processes by regulating downstream gene expression (35). In addition, MECOM is a tumour suppressor that plays an important role in normal development and tumourigenesis (36). Li *et al* (37) reported that in LUAD, the mRNA levels of MECOM are downregulated and that it may serve as a potential prognostic biomarker. In the present study, MECOM expression was downregulated in LUAD tissues. The ChIP assay confirmed that MECOM directly regulated the transcription of HSPB7 in LUAD. Furthermore, overexpression of MECOM inhibited proliferation, migration, invasion, glucose consumption and lactic acid production in lung cancer cells; while knockdown of HSPB7 attenuated the inhibitory effect of MECOM on cell behaviour. Taken together, these findings confirmed that HSPB7 was regulated by MECOM and participated in the progression of LUAD.

There were certain limitations to the present study. First, an *in vivo* metastatic assay was not performed. Secondly, the effect of HSPB7 on apoptosis remains unclear. Future studies could address these limitations.

In summary, HSPB7 was expressed at low levels in LUAD tissues and cells, and overexpression of HSPB7 inhibited lung cancer cell proliferation, invasion and migration. HSPB7 was regulated by the MECOM and inhibited LUAD progression by inhibiting glycolysis. The findings of the present study provide a new insight into HSPB7 expression in patients with LUAD.

Acknowledgements

Not applicable.

Funding

No funding was received.

Availability of data and materials

The datasets used and/or analyzed during the current study are available from the corresponding author on reasonable request.

Authors' contributions

ZTC conceived and designed the study. PPL, LGS and XYJ provided study materials. PPL, LGS and XYJ collected and assembled the data. ZTC analyzed and interpreted the data. LGS and XYJ confirm the authenticity of all the raw data. All authors participated in manuscript writing, read and approved the final version of the manuscript.

Ethics approval and consent to participate

The protocols of human studies (W202203060147) and animal experiments (W202203060148) were approved by the Ethics Committee of Jinan Central Hospital Affiliated to Shandong First Medical University (Jinan, China). Written informed consent was provided by all patients.

Patient consent for publication

Not applicable.

Competing interests

The authors declare that they have no competing interests.

References

1. Chen W, Zheng R, Baade PD, Zhang S, Zeng H, Bray F, Jemal A, Yu XQ and He J: Cancer statistics in China, 2015. CA Cancer J Clin 66: 115-132, 2016.
2. Kerdidani D, Chouvardas P, Arjo AR, Giopanou I, Ntaliarda G, Guo YA, Tsikitis M, Kazamias G, Potaris K, Stathopoulos GT, *et al*: Wnt1 silences chemokine genes in dendritic cells and induces adaptive immune resistance in lung adenocarcinoma. Nat Commun 10: 1405, 2019.
3. Zhao F, Zhao Z, Han Y, Li S, Liu C and Jia K: Baicalin suppresses lung cancer growth phenotypes via miR-340-5p/NET1 axis. Bioengineered 12: 1699-1707, 2021.
4. Hirsch FR, Scagliotti GV, Mulshine JL, Kwon R, Curran WJ Jr, Wu YL and Paz-Ares L: Lung cancer: Current therapies and new targeted treatments. Lancet 389: 299-311, 2017.
5. Liu Z, Sun D, Zhu Q and Liu X: The screening of immune-related biomarkers for prognosis of lung adenocarcinoma. Bioengineered 12: 1273-1285, 2021.
6. Gettinger S and Lynch T: A decade of advances in treatment for advanced non-small cell lung cancer. Clin Chest Med 32: 839-851, 2011.
7. Wang X, Shi B, Zhao Y, Lu Q, Fei X, Lu C, Li C and Chen H: HKDC1 promotes the tumorigenesis and glycolysis in lung adenocarcinoma via regulating AMPK/mTOR signaling pathway. Cancer Cell Int 20: 450, 2020.
8. Pagliarone AC, Castañeda ED, Santana JPP, de Oliveira CAB, Robeldo TA, Teixeira FR and Borra RC: Mitochondrial heat shock protein mortalin as potential target for therapies based on oxidative stress. Photodiagnosis Photodyn Ther 34: 102256, 2021.
9. Henstridge DC, Whitham M and Febbraio MA: Chaperoning to the metabolic party: The emerging therapeutic role of heat-shock proteins in obesity and type 2 diabetes. Mol Metab 3: 781-793, 2014.
10. Mymrikov EV, Riedl M, Peters C, Weinkauf S, Haslbeck M and Buchner J: Regulation of small heat-shock proteins by hetero-oligomer formation. J Biol Chem 295: 158-169, 2020.
11. Muranova LK, Shatov VM, Bukach OV and Gusev NB: Cardio-vascular heat shock protein (cvHsp, HspB7), an unusual representative of small heat shock protein family. Biochemistry (Mosc) 86 (Suppl 1): S1-S11, 2021.
12. Wu T, Mu Y, Bogomolovas J, Fang X, Veevers J, Nowak RB, Pappas CT, Gregorio CC, Evans SM, Fowler VM and Chen J: HSPB7 is indispensable for heart development by modulating actin filament assembly. Proc Natl Acad Sci USA 114: 11956-11961, 2017.
13. Juo LY, Liao WC, Shih YL, Yang BY, Liu AB and Yan YT: HSPB7 interacts with dimerized FLNC and its absence results in progressive myopathy in skeletal muscles. J Cell Sci 129: 1661-1670, 2016.
14. Liu CC, Chou KT, Hsu JW, Lin JH, Hsu TW, Yen DH, Hung SC and Hsu HS: High metabolic rate and stem cell characteristics of esophageal cancer stem-like cells depend on the Hsp27-AKT-HK2 pathway. Int J Cancer 145: 2144-2156, 2019.
15. Liu S, Yan B, Lai W, Chen L, Xiao D, Xi S, Jiang Y, Dong X, An J, Chen X, *et al*: As a novel p53 direct target, bidirectional gene HspB2/αB-crystallin regulates the ROS level and Warburg effect. Biochim Biophys Acta 7: 592-603, 2014.
16. Naderi A: SRARP and HSPB7 are epigenetically regulated gene pairs that function as tumor suppressors and predict clinical outcome in malignancies. Mol Oncol 12: 724-755, 2018.
17. Lin J, Deng Z, Tanikawa C, Shuin T, Miki T, Matsuda K and Nakamura Y: Downregulation of the tumor suppressor HSPB7, involved in the p53 pathway, in renal cell carcinoma by hypermethylation. Int J Oncol 44: 1490-1498, 2014.
18. Liu J, Lichtenberg T, Hoadley KA, Poisson LM, Lazar AJ, Cherniack AD, Kovatich AJ, Benz CC, Levine DA, Lee AV, *et al*: An integrated TCGA pan-cancer clinical data resource to drive high-quality survival outcome analytics. Cell 173: 400-416.e11, 2018.
19. Riaz SP, Horton M, Kang J, Mak V, Lüchtenborg M and Møller H: Lung cancer incidence and survival in England: An analysis by socioeconomic deprivation and urbanization. J Thorac Oncol 6: 2005-2010, 2011.
20. Livak KJ and Schmittgen TD: Analysis of relative gene expression data using real-time quantitative PCR and the 2(-Delta Delta C(T)) method. Methods 25: 402-408, 2001.
21. Wu XT, Wang YH, Cai XY, Dong Y, Cui Q, Zhou YN, Yang XW, Lu WF and Zhang M: RNF115 promotes lung adenocarcinoma through Wnt/β-catenin pathway activation by mediating APC ubiquitination. Cancer Metab 9: 7, 2021.
22. Sutula TP and Fountain NB: 2DG and glycolysis as therapeutic targets for status epilepticus. Epilepsy Behav 140: 109108, 2023.
23. Wang L, Wang H, Wu B, Zhang C, Yu H, Li X, Wang Q, Shi X, Fan C, Wang D, *et al*: Long noncoding RNA LINC00551 suppresses glycolysis and tumor progression by regulating c-Myc-mediated PKM2 expression in lung adenocarcinoma. Onco Targets Ther 13: 11459-11470, 2020.
24. Zhuo X, Chen L, Lai Z, Liu J, Li S, Hu A and Lin Y: Protein phosphatase 1 regulatory subunit 3G (PPP1R3G) correlates with poor prognosis and immune infiltration in lung adenocarcinoma. Bioengineered 12: 8336-8346, 2021.
25. Rocco D, Della Gravara L, Battiloro C, Maione P and Gridelli C: The treatment of advanced lung adenocarcinoma with activating EGFR mutations. Expert Opin Pharmacother 22: 2475-2482, 2021.
26. Lamberti G, Andrini E, Sisi M, Rizzo A, Parisi C, Di Federico A, Gelsomino F and Ardizzoni A: Beyond EGFR, ALK and ROS1: Current evidence and future perspectives on newly targetable oncogenic drivers in lung adenocarcinoma. Crit Rev Oncol Hematol 156: 103119, 2020.
27. Bezdenezhnykh N, Semesiuk N, Lykhova O, Zhylchuk V and Kudryavets Y: Impact of stromal cell components of tumor microenvironment on epithelial-mesenchymal transition in breast cancer cells. Exp Oncol 36: 72-78, 2014.
28. Cervantes-Arias A, Pang LY and Argyle DJ: Epithelial-mesenchymal transition as a fundamental mechanism underlying the cancer phenotype. Vet Comp Oncol 11: 169-184, 2013.
29. Becker KF, Rosivatz E, Blechschmidt K, Kremmer E, Sarbia M and Höfler H: Analysis of the E-cadherin repressor Snail in primary human cancers. Cells Tissues Organs 185: 204-212, 2007.
30. Ganapathy-Kanniappan S and Geschwind JF: Tumor glycolysis as a target for cancer therapy: Progress and prospects. Mol Cancer 12: 152, 2013.
31. Zhou J, Zhang S, Chen Z, He Z, Xu Y and Li Z: CircRNA-ENO1 promoted glycolysis and tumor progression in lung adenocarcinoma through upregulating its host gene ENO1. Cell Death Dis 10: 885, 2019.
32. Zhang L, Zhang Z and Yu Z: Identification of a novel glycolysis-related gene signature for predicting metastasis and survival in patients with lung adenocarcinoma. J Transl Med 17: 423, 2019.
33. Zhou L, Li M, Yu X, Gao F and Li W: Repression of hexokinases II-Mediated glycolysis contributes to piperlongumine-induced tumor suppression in non-small cell lung cancer cells. Int J Biol Sci 15: 826-837, 2019.
34. Ripperger T, Hofmann W, Koch JC, Shirneshan K, Haase D, Wulf G, Issing PR, Karnebogen M, Schmidt G, Auber B, *et al*: MDS1 and EVI1 complex locus (MECOM): A novel candidate gene for hereditary hematological malignancies. Haematologica 103: e55-e58, 2018.
35. Bleu M, Mermet-Meillon F, Apfel V, Barys L, Holzer L, Bachmann Salvy M, Lopes R, Amorim Monteiro Barbosa I, Delmas C, Hinniger A, *et al*: PAX8 and MECOM are interaction partners driving ovarian cancer. Nat Commun 12: 2442, 2021.
36. Germeshausen M, Ancliff P, Estrada J, Metzler M, Ponstingl E, Rütschle H, Schwabe D, Scott RH, Unal S, Wawer A, *et al*: MECOM-associated syndrome: A heterogeneous inherited bone marrow failure syndrome with amegakaryocytic thrombocytopenia. Blood Adv 2: 586-596, 2018.
37. Li M, Ren H, Zhang Y, Liu N, Fan M, Wang K, Yang T, Chen M and Shi P: MECOM/PRDM3 and PRDM16 serve as prognostic-related biomarkers and are correlated with immune cell infiltration in lung adenocarcinoma. Front Oncol 12: 772686, 2022.